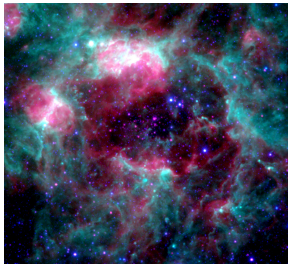


SOFIA/GREAT observations of LMC-N 11: Does [C II] trace regions with a large H₂ fraction?

Vianney Lebouteiller

Laboratoire AIM - CEA, Saclay, France

Main collaborators: F. Galliano, S. Madden, M. Chevance, F. Polles, M.-Y. Lee (CEA),
D. Cormier (ZAH), A. Hugues (OMP), M. Requeña-Torres (STScI)



Motivations

What diagnostics can [C II] 157 μm hold?

- Important cooling line, carries $\sim 0.1 - 5\%$ of L_{FIR}
- SFR tracer (e.g., de Looze+ 2014) – C II* also used in DLAs (Wolfe+ 2003)
- Diagnostic for physical conditions in PDR models ([C II], [O I] 63, 145 μm , L_{FIR})
- CO-dark molecular gas tracer (Madden+ 1997; Wolfire+ 2010)

Routinely detected at high- z

- Recent detections: e.g., Aravena+ 2016; Bañados+ 2015; Pentericci+ 2016; Bradac+ 2016

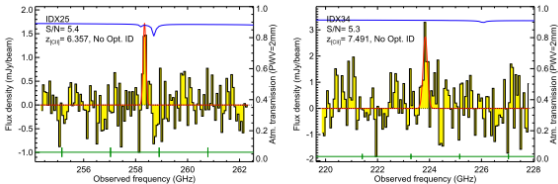


Fig.: $z > 6$ ALMA [C II] candidates with no optical counterparts in the Hubble-UDF; (Aravena+ 2016)

- Some surprising non-detections (e.g., Maiolino+ 2015; Carilli+) – AGN, low metallicity, significant absorption?

Motivations

What diagnostics can [C II] 157 μm hold?

- Important cooling line, carries $\sim 0.1 - 5\%$ of L_{FIR}
- SFR tracer (e.g., de Looze+ 2014) – C II* also used in DLAs (Wolfe+ 2003)
- Diagnostic for physical conditions in PDR models ([C II], [O I] 63, 145 μm , L_{FIR})
- CO-dark molecular gas tracer (Madden+ 1997; Wolfire+ 2010)

What is the origin of [C II]?

- CNM, WNM, PDR interfaces with molecular clouds, WIM
- Metal-poor ISM? Low dust abundance (increased PDR clumpiness, lower average A_V)

Previous studies

- **Milky Way** (Velusamy+ 2010; Piñeda+ 2012, 2015), **M 17-SW** (Pérez-Beaupuits+ 2015), **NGC 4214** (Fahrion+ 2016), **LMC-N 159** (Okada+ 2015), **SMC H II regions** (Requeña-Torres+ 2016)

- ⇒ [C II] traces significant CO-dark gas in star-forming regions (especially at low metallicity)
- ⇒ There might be significant [C II] not associated with the dense star-forming material

Scales and metallicity effects: **star-forming regions in Magellanic Clouds**

LMC-N 11

LMC

- $1/2 Z_{\odot}$
- Range of spatial scales

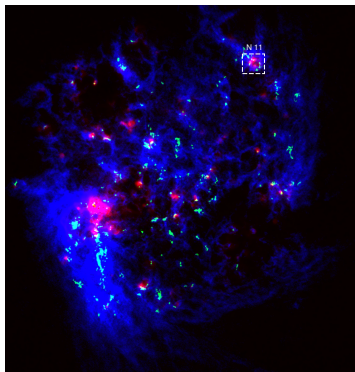


Fig.: LMC (R: $H\alpha$, G: CO(1-0) MAGMA, B: $H\text{ I } 21\text{ cm}$).

N 11

- Second largest $H\text{ II}$ region after 30 Dor ($\sim 120\text{ pc}$)
- At least 3 stellar generations



Fig.: N 11 (R: $H\alpha$, G: IRAC4 (PAH), B: IRAC1 (stars)).

Rich dataset & wide range of environments

SOFIA/GREAT: [C II] 157 μm and [N II] 205 μm

- 12 pointings previously identified as CO bright cores (MAGMA), [C II] bright spots (PACS)
- PDRs, quiescent CO cloud, ultracompact H II region, stellar cluster

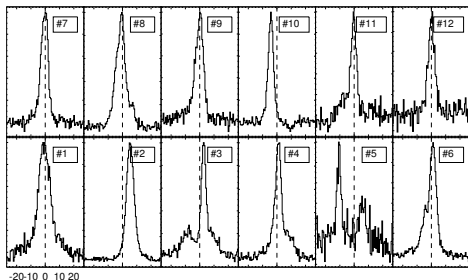


Fig.: [C II] spectra observed with GREAT.

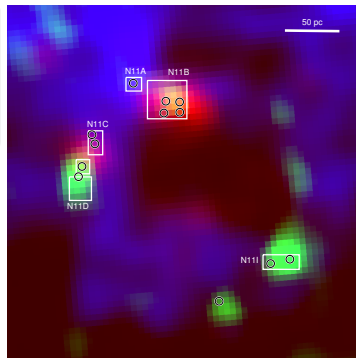


Fig.: N11 (R: H α , G: IRAC4 (PAH), B: IRAC1 (stars)).

& Herschel, Spitzer, CO(1-0)
MOPRA/MAGMA, CO(1-0) ALMA,
H I 21 cm ATCA+Parkes,
VLT/GIRAFFE...

Some comparisons

- *Herschel*/PACS [C II] fluxes lower by 1.5 on average (but point-source vs. extended-source flux calibration)

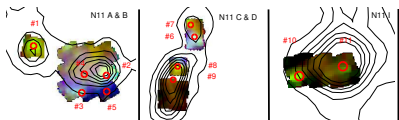


Fig.: PACS (R: [C II], G: [O I], B: [O III] 88 μ m) & CO(1-0).

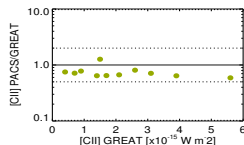


Fig.: Comparison of GREAT and PACS [C II] fluxes.

- ALMA CO(1-0) observation of N11B (PI Leboutteiller)

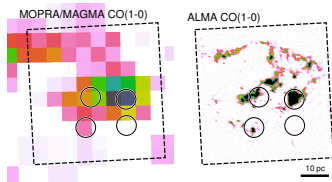


Fig.: MOPRA/MAGMA and ALMA CO(1-0) in N11B.

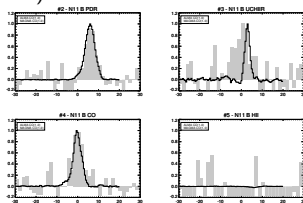
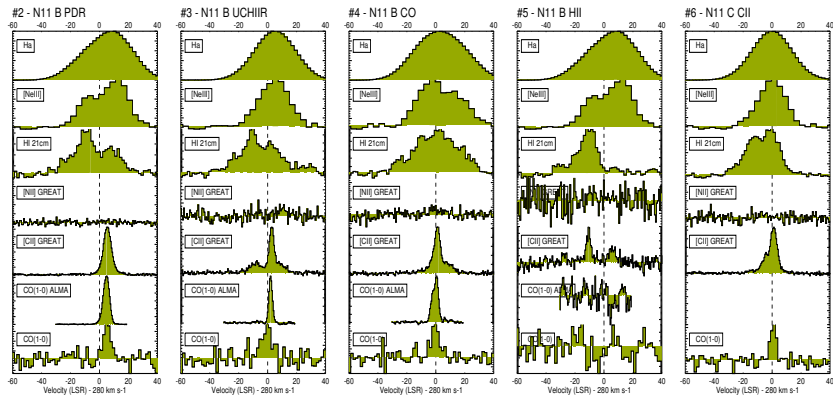


Fig.: MOPRA/MAGMA and ALMA CO(1-0) profiles.

Profiles



CO: usually a single component – FWHM $3 - 8 \text{ km s}^{-1}$

[C II]: more structure – (Total) FWHM $4 - 10 \text{ km s}^{-1}$

H I: even more structure – (Total) FWHM $16 - 40 \text{ km s}^{-1}$

H α and [Ne III] $\lambda 3868$: 15 km s^{-1} resolution, kinematic (non-thermal) width $15 - 25 \text{ km s}^{-1}$.

[C II] in the ionized gas

Integrated measurement: $[C II] + [O I] / PAH$ (PACS+Spitzer)

- Gas cooling / gas heating (PE), probe of PE heating efficiency (Helou+ 2001; Croxall+ 2012; Lebouteiller+ 2012; Okada+ 2013)
- Remarkably tight ratio across N 11. No regions with significantly larger ratio than PDR-dominated regions

Integrated measurement: $[N II] / [C II]$ (PACS)

- Integrated ratios $[N II]_{122, 205 \mu m} / [C II]$ ($\lesssim 0.05, 0.02$) much lower than theoretical ratio in ionized gas

Line width for resolved components (GREAT)

- Width $<$ thermal broadening for C^+ in ionized gas (7 km s^{-1}). Exceptions: multiple components and one component toward #5

$[N II] 205 \mu m$ profile (GREAT)

- Expected $[N II] 205 \mu m$ profile assuming $[C II]$ originates fully from the ionized gas \gg observed upper limit
- Again one possible exception toward #5 (where the $[C II]$ fraction in the ionized gas is $\lesssim 2/3$)

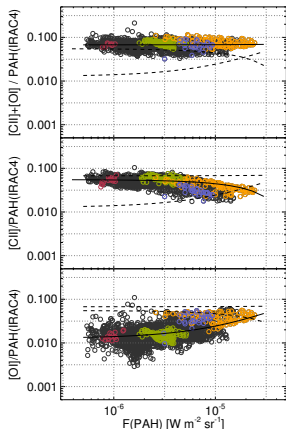


Fig.: $[O I] / PAH$ (bottom), $[C II] / PAH$ (middle) and $[C II] + [O I] / PAH$ (top) vs. PAH flux.

[C II] in the ionized gas

Integrated measurement: [C II]+[O I]/PAH (PACS+Spitzer)

- Gas cooling / gas heating (PE), probe of PE heating efficiency (Helou+ 2001; Croxall+ 2012; Lebouteiller+ 2012; Okada+ 2013)
- Remarkably tight ratio across N 11. No regions with significantly larger ratio than PDR-dominated regions

Integrated measurement: [N II]/[C II] (PACS)

- Integrated ratios [N II]_{122, 205 μm}/[C II] ($\lesssim 0.05, 0.02$) much lower than theoretical ratio in ionized gas

Line width for resolved components (GREAT)

- Width < thermal broadening for C⁺ in ionized gas (7 km s^{-1}). Exceptions: multiple components and one component toward #5

[N II] 205 μm profile (GREAT)

- Expected [N II] 205 μm profile assuming [C II] originates fully from the ionized gas >> observed upper limit
- Again one possible exception toward #5 (where the [C II] fraction in the ionized gas is $\lesssim 2/3$)

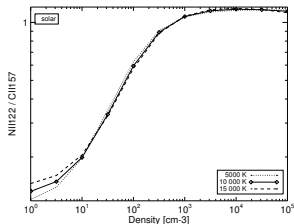
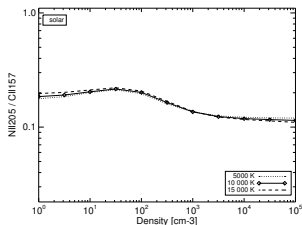


Fig.: Theoretical [N II]/[C II] in the ionized gas.

[C II] in the ionized gas

Integrated measurement: [C II]+[O I]/PAH (PACS+Spitzer)

- Gas cooling / gas heating (PE), probe of PE heating efficiency (*Helou+ 2001; Croxall+ 2012; Lebouteiller+ 2012; Okada+ 2013*)
- Remarkably tight ratio across N11. No regions with significantly larger ratio than PDR-dominated regions

Integrated measurement: [N II]/[C II] (PACS)

- Integrated ratios [N II]_{122, 205 μ m}/[C II] ($\lesssim 0.05, 0.02$) much lower than theoretical ratio in ionized gas

Line width for resolved components (GREAT)

- Width < thermal broadening for C⁺ in ionized gas (7 km s⁻¹). Exceptions: multiple components and one component toward #5

[N II] 205 μ m profile (GREAT)

- Expected [N II] 205 μ m profile assuming [C II] originates fully from the ionized gas >> observed upper limit
- Again one possible exception toward #5 (where the [C II] fraction in the ionized gas is $\lesssim 2/3$)

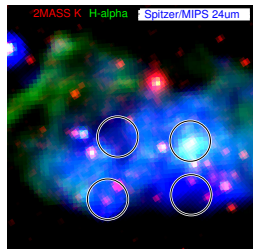
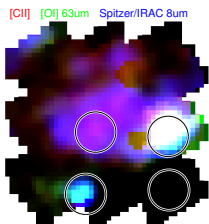


Fig.: Pointing #5 observes toward stellar cluster LH10, dominated by [O III], 24 μ m, H α emission.

[C II] in the ionized gas

Integrated measurement: [C II]+[O I]/PAH (PACS+Spitzer)

- Gas cooling / gas heating (PE), probe of PE heating efficiency (Helou+ 2001; Croxall+ 2012; Leboutteiller+ 2012; Okada+ 2013)
- Remarkably tight ratio across N11. No regions with significantly larger ratio than PDR-dominated regions

Integrated measurement: [N II]/[C II] (PACS)

- Integrated ratios [N II]_{122, 205 μ m}/[C II] (\lesssim 0.05, 0.02) much lower than theoretical ratio in ionized gas

Line width for resolved components (GREAT)

- Width < thermal broadening for C⁺ in ionized gas (7 km s⁻¹). Exceptions: multiple components and one component toward #5

[N II] 205 μ m profile (GREAT)

- Expected [N II] 205 μ m profile assuming [C II] originates fully from the ionized gas \gg observed upper limit
- Again one possible exception toward #5 (where the [C II] fraction in the ionized gas is \lesssim 2/3)

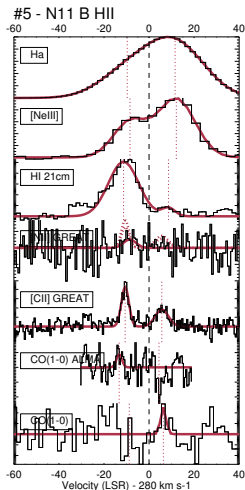


Fig.: One component toward pointing #5 could be associated with H I or with the ionized gas.

[C II] in the ionized gas

Integrated measurement: [C II]+[O I]/PAH (PACS+Spitzer)

- Gas cooling / gas heating (PE), probe of PE heating efficiency (Helou+ 2001; Croxall+ 2012; Lebouteiller+ 2012; Okada+ 2013)
- Remarkably tight ratio across N11. No regions with significantly larger ratio than PDR-dominated regions

Integrated measurement: [N II]/[C II] (PACS)

- Integrated ratios [N II]_{122, 205 μm}/[C II] ($\lesssim 0.05, 0.02$) much lower than theoretical ratio in ionized gas

Line width for resolved components (GREAT)

- Width < thermal broadening for C⁺ in ionized gas (7 km s⁻¹). Exceptions: multiple components and one component toward #5

[N II] 205 μm profile (GREAT)

- Expected [N II] 205 μm profile assuming [C II] originates fully from the ionized gas \gg observed upper limit
- Again one possible exception toward #5 (where the [C II] fraction in the ionized gas is $\lesssim 2/3$)

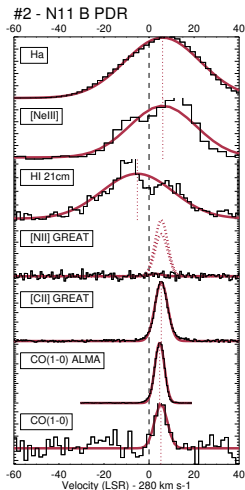


Fig.: [C II] originates from the neutral medium in most if not all components toward all pointings.

[C II] decomposition method (1/2): $\text{CO} \rightarrow [\text{C II}] \rightarrow \text{H I}$

- Fitting increasingly complex profiles and add (as few) components as necessary
- Always a [C II] component with same velocity and width as the CO component
- \Rightarrow [C II] appears wider because of multiple components (not because of larger-scale envelope around CO emitting-region)

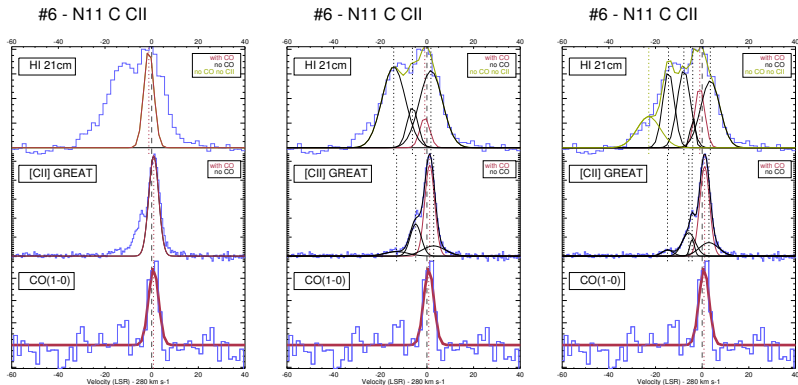
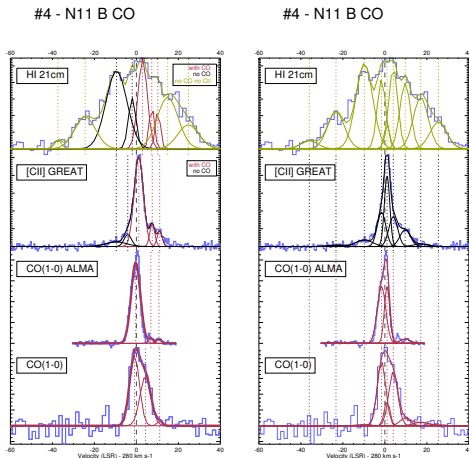


Fig.: The number of necessary components increases from CO to [C II] to H I.

[C II] decomposition method (2/2): simultaneous fit

- The minimum number of components identified in CO, [C II], and H I are now fed back to all the tracers \Rightarrow **Individual component properties**



Statistics on components

Regimes

- No bright [C II] components with low $f(\text{H}_2)$ (as derived from CO)
- Two main regimes
 - Bright, narrow, [C II] components with large $f(\text{H}_2)$
 - Faint, broad, [C II] components with low $f(\text{H}_2)$
- Some components with moderately bright [C II] components & low $f(\text{H}_2)$ \Rightarrow Candidates for CO-dark molecular or atomic gas

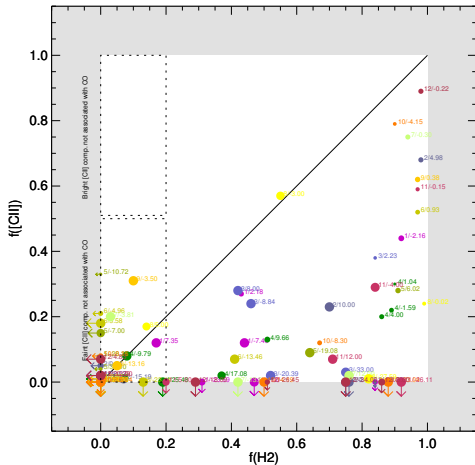


Fig.: Fraction of [C II] in component vs. molecular gas fraction. Size of symbol \propto component line width.

Theoretical expectations

Method

- Calculate theoretical [C II] intensity for collisions with H^0 , e^- , and H_2
- Using observed column densities of individual components for H^0 and H_2
 - *Allowing 10× more to accommodate for low spatial resolution ($H\text{ I}$ and CO) or for dense PDRs not well traced by $H\text{ I } 21\text{ cm}$*
- Two phases: neutral atomic $n(H^0) = 500\text{ cm}^{-3}$, and molecular $n(H_2) = 10^{3-4}\text{ cm}^{-3}$
- Using $6 \times 10^{20}\text{ K km s}^{-1}\text{ cm}^{-2}$ for X_{CO} (Roman-Duval+ 2014)

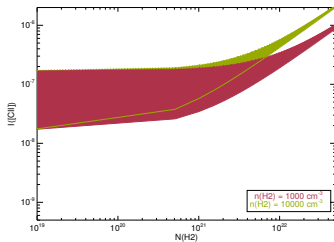
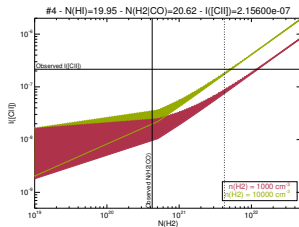
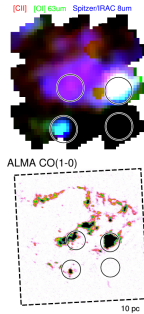


Fig.: Expected [C II] line intensity for given H^0 , H_2 column densities and volume densities.

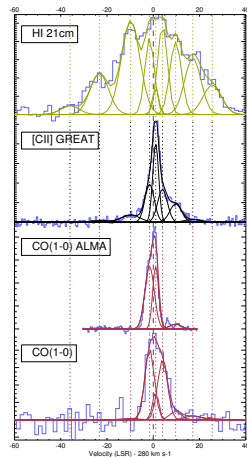
Theoretical expectations

Results

- Many [C II] components associated with CO require either **much larger column densities (dense PDRs / CO-dark gas)**
- Collisions with H_2 dominate there + discrepancy even using ALMA (high) column densities \Rightarrow CO-dark gas?



#4 - N11 B CO



“Well-behaved” clouds

- Some pointings (#9, #11, #12, #7, and #8), *despite being CO bright*, do not have any component that requires extra density and/or CO-dark gas
- Common property: **quiescent CO clouds**
- ⇒ Indirect evidence of CO-dark gas in other pointings due to presence of massive stars

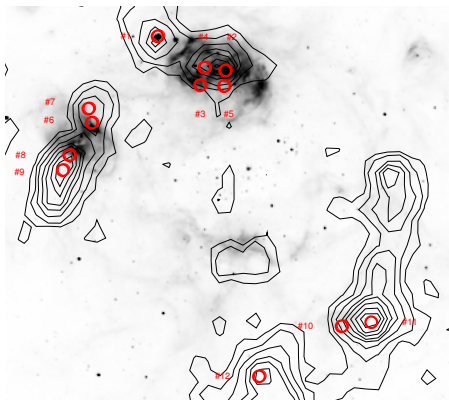
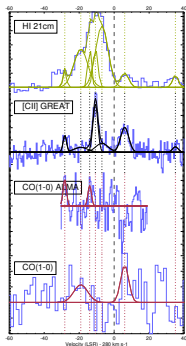


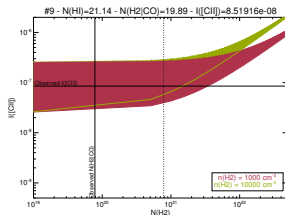
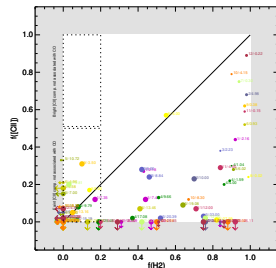
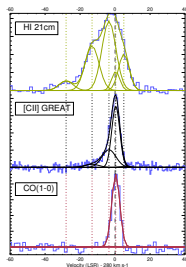
Fig.: $H\alpha$ image of LMC-N 11, with CO(1-0) contours.

- Weak [C II] components not associated with (bright) CO are compatible with theoretical calculation
- Collisions with H^0 are enough for these components ([C II] in CNM candidate?) – interestingly hard to probe in more distant sources, beam effect? (Fahrion+ 2016)

#5 - N11 B HII



#9 - N11 D



Prospectives

Observations

- Entire region scale: what phases dominate and what is the fraction of CO-dark gas? \Rightarrow mapping capabilities of upGREAT
- Ionized gas contamination \Rightarrow deeper [N II] $205 \mu\text{m}$, new [O I] $63 \mu\text{m}$ – H α – radio continuum – H radio recombination line (*Pérez-Beaupuits+ 2015*)

Calculations

- Decomposition tricky, no unique solution but some robustness for results
- PDR models to improve the (naive) theoretical predictions – H I 21 cm favors the lower density gas
- What cools the H I components not seen in [C II]? Very diffuse gas with [C II] too faint?
- LMC only $1/2 Z_{\odot}$. Lower metallicities need to be explored for effects on the CO-dark gas (but at extremely low metallicities, photoelectric effect may not dominate anymore)

Summary

SOFIA/GREAT observations of [C II] and [N II] $205\ \mu\text{m}$ in LMC-N 11

- **No evidence of [C II] in the ionized gas (only one exception, maybe)**
- **Most of the [C II] is associated with components with large $f(\text{H}_2)$**
- **The brightest [C II] component toward all pointing is always associated with CO, with similar velocity and width**
 - Theoretical calculations suggest that most [C II] bright components associated with CO require either CO-dark gas or significantly larger column densities
 - Consistent with large X_{CO} factor calculated in 30 Dor? (*Chevanche+ 2016*)
- **Some [C II] components associated with CO are ok with theoretical calculation**
 - Quiescent CO clouds
- **Several extra components seen in [C II], some seem to be associated with H I. Usually relatively broad.**
 - Most extra components agree with theoretical expectations (CNM faint components?)

END – extra slides

SOFIA/GREAT vs. *Herschel*/PACS

All except one pointing observed with *Herschel*/PACS (SHINING program).

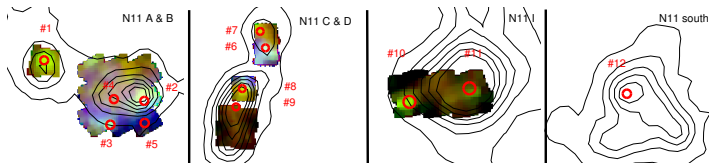


Fig.: PACS observations [C II] in red, [O I] in green, and [O III] 88 μm in blue. CO(1-0 contours)

[C II] 157 μm

- PACS fluxes lower by $\sim 50\%$ on average
- Caveat #1: using 14.1" for HPBW as measured in 2014, i.e., assuming observations are close to diffraction limit
- Caveat #2: Flux calibration extended/point-source

[N II] 205 μm

- Upper limits with GREAT and PACS

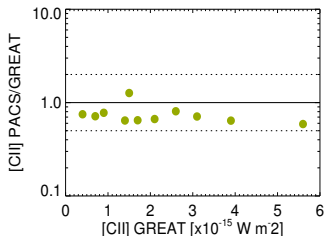


Fig.: Comparison of GREAT and PACS [C II] fluxes.

CO(1-0) observations in N 11B

- ALMA CO(1-0) observation (PI Lebouteiller)
- Drastic improvement of S/N and velocity resolution, especially toward stellar cluster where [C II] is detected
- Good agreement with MAGMA (matched to 45")

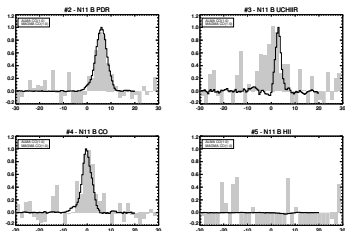


Fig.: Comparison of MOPRA/MAGMA and ALMA CO(1-0) maps in N 11B.

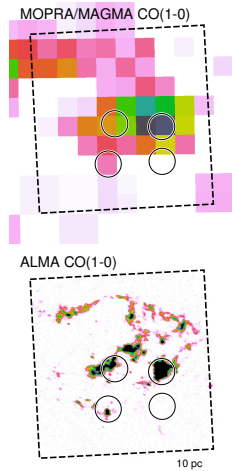


Fig.: Comparison of MOPRA/MAGMA and ALMA CO(1-0) maps in N 11B.

[C II] in the ionized gas

[N II]/[C II] intensity ratio with PACS

- *Integrated ratios* [N II]_{122 μm}/[C II] ($\lesssim 0.05$) and [N II]_{205 μm}/[C II] ($\lesssim 0.02$) much lower than theoretical ratio in ionized gas \Rightarrow most [C II] arises from neutral gas

Thermal broadening

- Expected thermal broadening for C⁺ in ionized gas: $\approx 7 \text{ km s}^{-1}$.
- Observed $< 7 \text{ km s}^{-1}$, except for pointings with multiple components and for one resolved component toward pointing #5

[N II] 205 μm with GREAT

- We calculate the expected [N II] 205 μm *profile* assuming [C II] originates fully from the ionized gas
- **No significant evidence of ionized gas contamination**, except maybe toward #5 (where the [C II] fraction in the ionized gas is $\lesssim 2/3$)

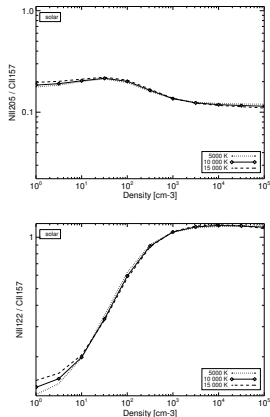


Fig.: Theoretical [N II]/[C II] in the ionized gas.]

[C II] in the ionized gas

[N II]/[C II] intensity ratio with PACS

- Integrated ratios $[N II]_{122 \mu m} / [C II]$ ($\lesssim 0.05$) and $[N II]_{205 \mu m} / [C II]$ ($\lesssim 0.02$) much lower than theoretical ratio in ionized gas \Rightarrow most [C II] arises from neutral gas

Thermal broadening

- Expected thermal broadening for C^+ in ionized gas: $\approx 7 \text{ km s}^{-1}$.
- Observed $< 7 \text{ km s}^{-1}$, except for pointings with multiple components and for one resolved component toward pointing #5

[N II] 205 μm with GREAT

- We calculate the expected [N II] 205 μm profile assuming [C II] originates fully from the ionized gas
- No significant evidence of ionized gas contamination, except maybe toward #5 (where the [C II] fraction in the ionized gas is $\lesssim 2/3$)

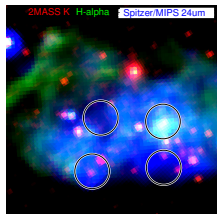
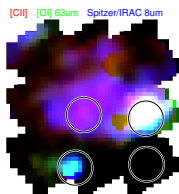


Fig.: Pointing #5 probes a region toward the stellar cluster LH10 dominated by [O III], 24 μm , H α emission.

[C II] in the ionized gas

[N II]/[C II] intensity ratio with PACS

- *Integrated ratios* $[N II]_{122 \mu m} / [C II]$ ($\lesssim 0.05$) and $[N II]_{205 \mu m} / [C II]$ ($\lesssim 0.02$) much lower than theoretical ratio in ionized gas \Rightarrow **most [C II] arises from neutral gas**

Thermal broadening

- Expected thermal broadening for C^+ in ionized gas: $\approx 7 \text{ km s}^{-1}$.
- Observed $< 7 \text{ km s}^{-1}$, except for pointings with multiple components and for one resolved component toward pointing #5

[N II] 205 μm with GREAT

- We calculate the expected [N II] 205 μm *profile* assuming [C II] originates fully from the ionized gas
- **No significant evidence of ionized gas contamination**, except maybe toward #5 (where the [C II] fraction in the ionized gas is $\lesssim 2/3$)

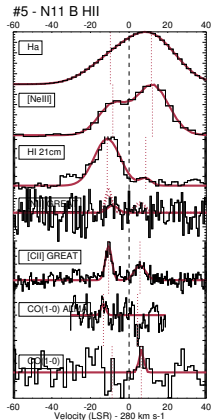


Fig.: One component toward pointing #5 could be associated with H I or with the ionized gas.

[C II] in the ionized gas

[N II]/[C II] intensity ratio with PACS

- *Integrated* ratios $[N II]_{122\ \mu m}/[C II]$ ($\lesssim 0.05$) and $[N II]_{205\ \mu m}/[C II]$ ($\lesssim 0.02$) much lower than theoretical ratio in ionized gas \Rightarrow most [C II] arises from neutral gas

Thermal broadening

- Expected thermal broadening for C^+ in ionized gas: $\approx 7\ \text{km s}^{-1}$.
- Observed $< 7\ \text{km s}^{-1}$, except for pointings with multiple components and for one resolved component toward pointing #5

[N II] 205 μm with GREAT

- We calculate the expected [N II] 205 μm profile assuming [C II] originates fully from the ionized gas
- No significant evidence of ionized gas contamination, except maybe toward #5 (where the [C II] fraction in the ionized gas is $\lesssim 2/3$)

\Rightarrow Contamination of [C II] in the ionized gas is unlikely, even for individual components

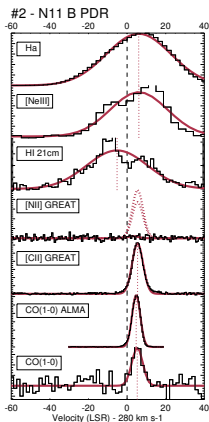


Fig.: [C II] originates from the neutral medium in most if not all components toward all pointings.

[C II]+[O I]/PAH

Photoelectric efficiency (PE)

- Ratio [C II]+[O I]/PAH as probe of PE heating efficiency (*Helou+ 2001; Croxall+ 2012; Lebouteiller+ 2012; Okada+ 2013*)
- Gas cooling in neutral gas: [C II] + [O I] (+...)
- Gas heating (PE): PAH or FIR
- Remarkably tight [C II]+[O I]/PAH across N11. No regions with significantly larger ratio than PDR-dominated regions
- ⇒ Circumstantial evidence that *integrated* [C II] arises from the neutral gas

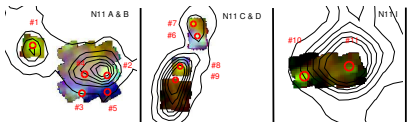


Fig.: PACS observations [C II] in red, [O I] in green, and [O III] 88 μm in blue. CO(1-0 contours)

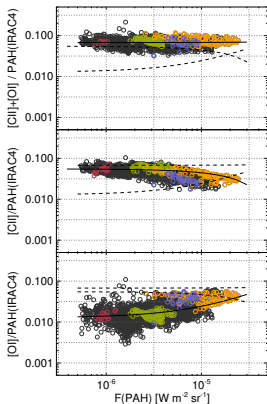


Fig.: [O I]/PAH (bottom), [C II]/PAH (middle) and [C II]+[O I]/PAH vs. PAH flux.

H I

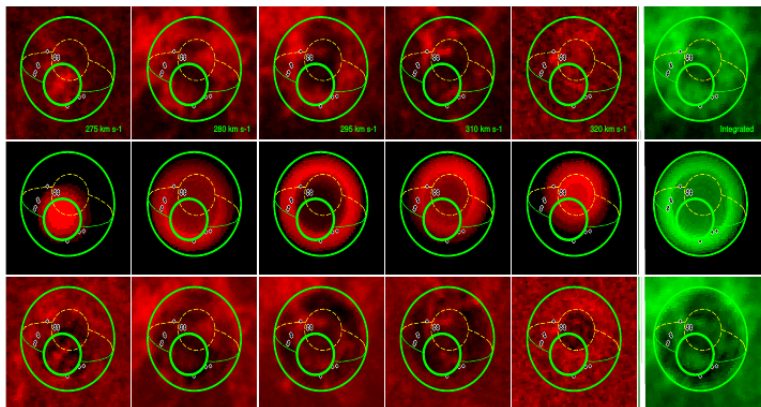
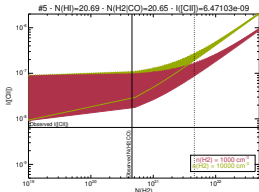
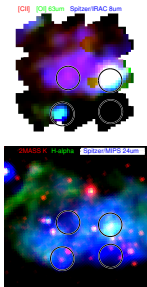


Fig. 5. H I cube at different velocity cuts. The rightmost panel shows the integrated flux. The top row shows the observed H I, the middle row shows a simple model as an expanding shell, and the bottom panel shows the residuals.

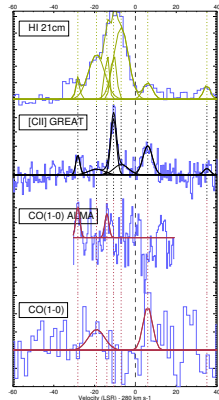
Theoretical expectations

Results

- Brightest [C II] components usually require either much larger column densities and/or volume densities. CO-dark gas is also a plausible explanation.
- Multiple high column-density components in beam not always an issue
- Low densities sometimes required, e.g., for all components toward #5



#5 - N11 B HII



Summary of data

| Instrument | Tracer | LSF FWHM [km s^{-1}] | PSF FWHM [$''$] |
|-----------------------|-----------------------|------------------------------------|------------------------------|
| SOFIA/GREAT | [C II], [N II] | 1.2 | $\approx 14.1, \approx 19.1$ |
| <i>Herschel</i> /PACS | [C II], [N II], ... | 250 | 12 |
| MAGMA | CO(1-0) | 0.53 | 45 |
| ALMA | CO(1-0) | 0.1 | 2 |
| ATCA+Parkes | H I 21 cm | 1.6 | 60 |
| VLT/GIRAFFE | H α , [Ne III] | 17, 15 | ≈ 1 |